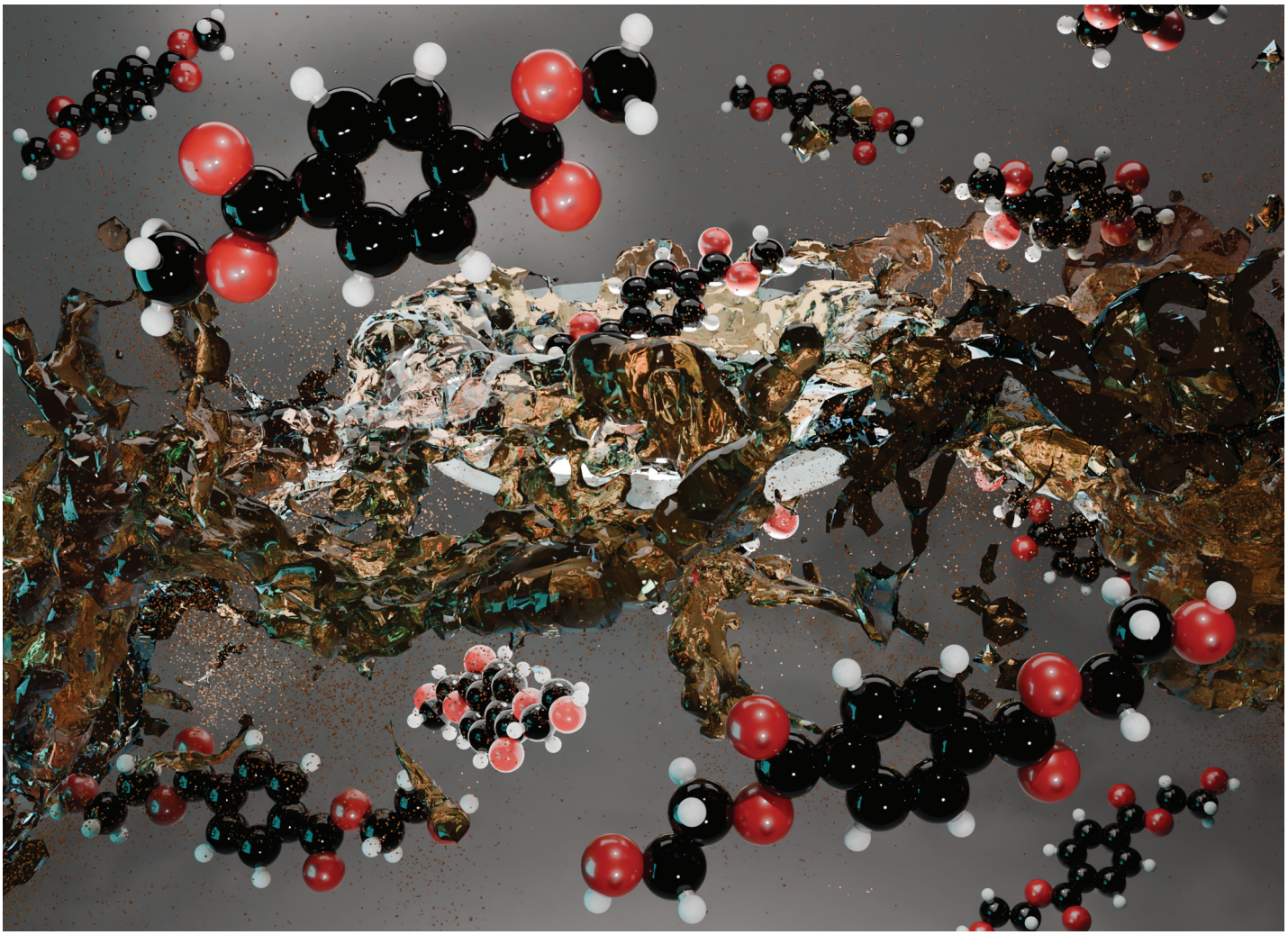

Showcasing research from Oak Ridge National Laboratory, Chemical Sciences Division, Tennessee, USA.

Upcycling of polyethylene terephthalate to high-value chemicals by carbonate-interchange deconstruction

Chemical upcycling could transform waste plastic into valuable feedstocks for chemical manufacturing. We report an efficient carbonate-based solvolysis process to convert waste PET into value-added terephthalate compounds at significantly reduced solvent demand compared with state-of-the-art methods.

Image reproduced by permission of Philip Gray (Artist) and Oak Ridge National Laboratory (ORNL) from *Green Chem.*, 2025, **27**, 15124.

As featured in:

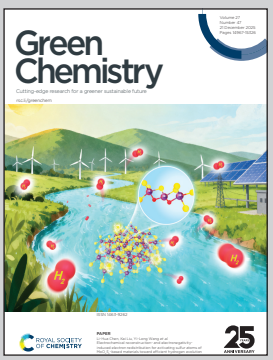

See Tomonori Saito, Jeffrey C. Foster *et al.*, *Green Chem.*, 2025, **27**, 15124.

ROYAL SOCIETY OF CHEMISTRY

rsc.li/greenchem

Registered charity number: 207890

Green Chemistry

PAPER

View Article Online
View Journal | View Issue

Cite this: *Green Chem.*, 2025, **27**, 15124

Upcycling of polyethylene terephthalate to high-value chemicals by carbonate-interchange deconstruction†

Nicholas J. Galan,[a] Isaiah T. Dishner,[a] Bobby G. Sumpter,[b] Vilmos Kertesz,[c] Nabihan B. Abdul Rahman,[a] Felipe Polo-Garzon,[a] Zoriana Demchuk,[a] Tomonori Saito *[a] and Jeffrey C. Foster *[a]

Received 1st July 2025,
Accepted 31st August 2025

DOI: 10.1039/d5gc03354c

rsc.li/greenchem

Condensation thermoplastics have become ubiquitous. The emergence of chemical upcycling could transform them into valuable feedstocks for chemical manufacturing at their end-of-life. However, current solvolysis processes suffer equilibrium limitations due to the liberation of reactive byproducts. We report a carbonate interchange deconstruction (CID) methodology for poly(ethylene terephthalate) (PET), where carbonates act as both latent nucleophiles and byproduct sequestering agents. High product selectivity (>95%) is achieved regardless of the targeted terephthalate product, originating from removal of ethylene glycol from the reaction equilibrium *via* its conversion into various oligoethers. CID is robust to the impurities present in post-consumer waste plastics and significantly reduces solvent demand, with just 10 mL of dimethyl carbonate successfully converting *ca.* 5 g of mixed PET waste into highly pure dimethyl terephthalate in excellent isolated yield (92%). CID opens a new upcycling paradigm wherein CO_2, embedded in carbonates, is leveraged to choreograph the selectivity of an otherwise equilibrium-controlled polymer upcycling process.

Green foundation

1. We present a carbonate-interchange deconstruction methodology for PET, a major environmental pollutant, where carbonates, which can be prepared from biomass, act as both latent nucleophiles and byproduct sequestering agents to afford valuable terephthalates small molecules at relatively mild conditions.
2. High product selectivity is attained with minimal excess of carbonate. This significantly reduces solvent demand compared with traditional alcoholysis methods.
3. Future research will focus on direct preparation of carbonates from CO_2 captured from the recycling process.

Introduction

Condensation polymers such as poly(ethylene terephthalate) (PET) are an important class of commodity thermoplastic materials characterized by their low cost, good barrier properties, and high strength-to-weight ratios, among other desirable features. Such materials are indispensable in a broad range of commercial and industrial applications and account for *ca.* 37% of the global polymer market size, with a valuation of *ca.* 268 billion USD and a projected valuation of 377 billion by 2030.[1–4] Despite their prevalence, most condensation polymers are not recycled due to difficulties in treating their various forms by conventional mechanical recycling.[5] The generally limited recycling of plastics (*ca.* 9% annually)[6] drives their accumulation in the environment and, crucially, wastes the feedstock resources and energy invested in their production. Developing generic and profitable strategies to convert waste plastics into useful chemicals and materials while providing increased value compared to virgin monomers is a desirable end-of-life strategy.[7–10]

Traditional chemical recycling methods have focused on regenerating the polymer's constituent monomers (*e.g.*, dimethyl terephthalate, **DMT**, from PET), offering little cost

[a]*Chemical Sciences Division, Oak Ridge National Laboratory, Oak Ridge, TN 37821, USA. E-mail: fosterjc@ornl.gov, saitot@ornl.gov*
[b]*Center for Nanophase Materials Sciences, Oak Ridge National Laboratory, Oak Ridge, TN 37821, USA*
[c]*Biosciences Division, Oak Ridge National Laboratory, Oak Ridge, TN 37821, USA*

benefit relative to the production of the virgin materials. To date, only a handful of studies have focused on upcycling condensation thermoplastics to organic compounds beyond monomers. Salient examples include transition metal catalyzed hydrogenation of PET to afford multifunctional small molecules such as 1,4-benzenedimethanol,[11] or hydrogen-free reductions to various aromatic species such as benzene, toluene, and xylene.[12] Inspired by this precedent, we envisioned that chemical deconstruction of PET by transesterification could offer a pathway to valuable terephthalate-based compounds beyond PET monomers **DMT** or bis(2-hydroxyethyl) terephthalate (**BHET**). Other small molecule terephthalates also have significant commercial relevance. For example, dibutyl terephthalate (**DBT**) and dioctyl terephthalate (**DOT**) are used as plasticizers in packaging, vinyl flooring, and other commercial materials. Diallyl terephthalate (**DAT**) is a key ingredient in resins for optical devices, is used as a reactive dilutant in unsaturated polyester resins, and is also commonly employed as a plasticizer, particularly for polyvinyl chloride (PVC). Dibenzyl terephthalate (**DBnT**) can also be used as a plasticizer or as an alternative to **DMT** or **BHET** in polyester synthesis. In addition to these examples, terephthalate compounds have found growing use in specialized applications such phase-change materials or crosslinked resins;[13–15] however, the preparation of such compounds directly from PET is underexplored. A recent report from our group detailed the preparation of α,ω-bis-alkenyl terephthalates from PET alcoholysis;[16] this work, along with related alcoholysis chemical upcycling methods, reinforced the equilibrium limitations of transesterification.[17] Put simply, solvolysis reactions must be conducted using a vast excess of alcoholic solvent to drive the reaction equilibrium towards the desired deconstruction product (Fig. 1, Top). The feasibility of solvolysis is therefore limited when the cost of the alcohol is prohibitive, or the alcohol exhibits dubious toxicity, (*e.g.*, methanol or allyl alcohol). Thus, there is significant motivation to unveil pathways for controlling transesterification reaction equilibria to enable new chemical upcycling approaches that selectively produce valuable organic compounds from waste condensation polymers.

We report the selective deconstruction of PET to value-added terephthalates using organic carbonates as a reaction medium (Fig. 1, Bottom). We hypothesized that carbonates alone, without the addition of alcohol and at near stoichiometric loadings, could be broadly exploited as a platform for PET deconstruction, enabling efficient and selective chemical upcycling to produce valuable terephthalate compounds beyond monomers. Our approach leverages the unique reactivity of carbonates, specifically their capacity to act as alkylating agents (*via* $B_{AL}2$ reactions) and convert alcohols to ethers in irreversible fashion.[18] In the context of PET deconstruction, this unique reactivity drives the transesterification equilibrium towards the desired terephthalate products through irreversible consumption (*via* alkylation) of evolving ethylene glycol

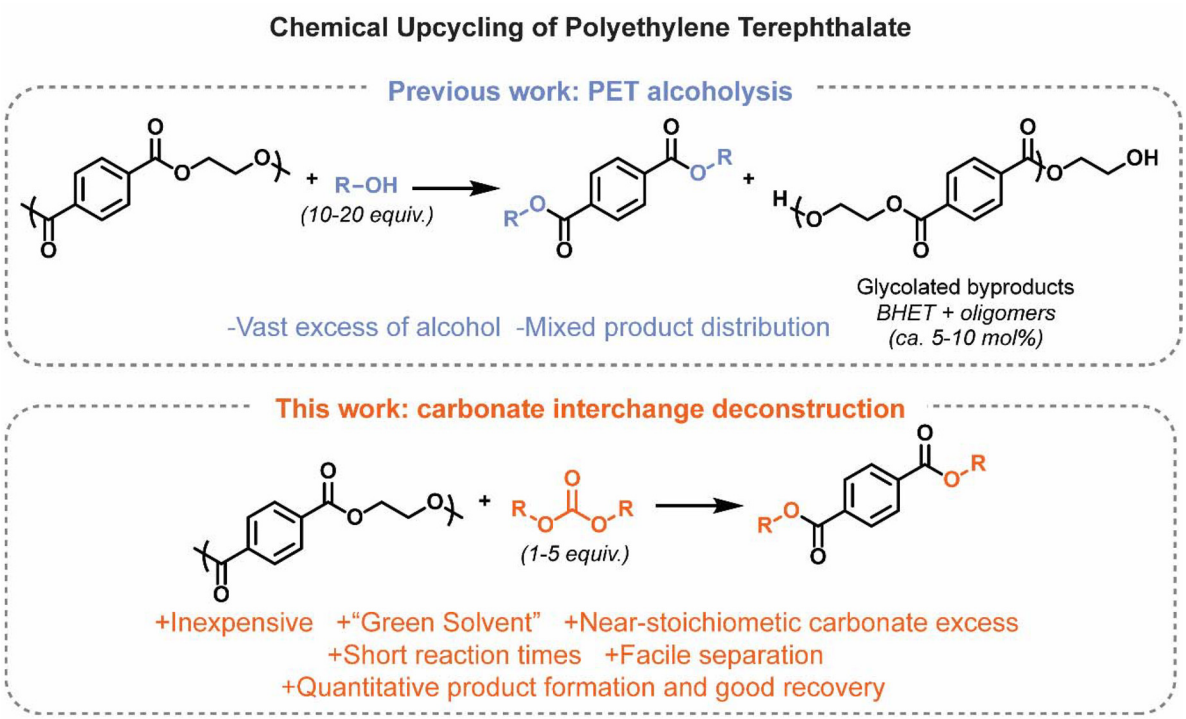

Fig. 1 (Top) PET deconstruction *via* alcoholysis currently requires vast excesses of alcohol and produces glycolated byproducts. (Bottom) The use of carbonates in place of alcohols for PET deconstruction significantly reduces solvent excess, affording high isolated yields of valuable terephthalate products.

(EG). Chemical deconstruction of PET using various carbonates was found to occur selectively with as little as 1 molar equiv. of carbonate, affording high yields of functional terephthalate compounds. This methodology was robust to impurities in post-consumer materials and could be deployed to deconstruct a variety of PET sources. Our process provides an alternative to alcoholysis, producing valuable terephthalates such as **DBT**, **DOT**, **DAT**, and **DBnT** at much lower temperatures, pressures, and solvent volumes than traditional methods. Based on the high selectivity of this carbonate interchange deconstruction (CID), the low cost and commercial availability of organic carbonates, and their growing sustainability profile, we envision our strategy will have significant economic and environmental impact, enabling the utilization of waste condensation polymers as synthetic feedstocks while combatting their accumulation in the environment.

Experimental

Materials

All chemicals were purchased from commercial sources and used as received unless stated otherwise. TBD/TFA was prepared in accordance with the literature procedure.[26]

Representative polymer carbonate-interchange deconstruction protocol. A 15 mL thick-walled glass pressure tube was charged with PET pellets (2.6 mmol, 1 equiv.), catalyst (0.01–0.1 equiv.), a PTFE coated stir bar, and carbonate (2–20 equiv.). The tube was tightly sealed, and the reaction mixture was heated to 180 °C in an oil bath with vigorous stirring. After a prescribed reaction time, the pressure tube was removed from heat and allowed to cool to room temperature. The cap was unscrewed to release the pressure, resulting in significant bubbling. The crude reaction mixture was sampled for analysis by ^{1}H NMR spectroscopy. The various terephthalate products were isolated as described in the SI.

Characterization methods

NMR spectroscopy. ^{1}H and ^{13}C NMR spectra were recorded on a Bruker Avance III 400 NMR spectrometer operating at 400 MHz, or a Bruker Ascend Evo 400 spectrometer operating at 400 MHz equipped with a SampleCase autosampler carousel. Chemical shifts are reported in parts per million (ppm) relative to residual protonated solvent for ^{1}H ($CHCl_3$, δ = 7.26) and relative to carbon resonances of the solvent for ^{13}C ($CDCl_3$, δ = 77.16). Peak multiplicities are annotated as follows: app = apparent, br = broad, s = singlet, d = doublet, dd = doublet of doublets, t = triplet, q = quartet, p = quintet, m = multiplet.

Size exclusion chromatography. Size exclusion chromatography (SEC) analysis was performed on an Agilent 1260 Infinity II LC system equipped an Agilent MiniMIX-C Guard column (PL Gel 5 μM, 50 × 4.6 mm) and two Agilent PL HFIPgel (250 × 4.6 mm, 9 μm). The mobile phase used was HFIP at a flow rate of 0.3 mL min^{-1} (an Agilent EasiVial PMMA standard, containing 4 discrete molecular weights, was used for calibration). Detection was conducted using a differential refractive index (RI) detector, a light scattering detector operating with two angles at 90° and 15°. Number-average molecular weights (M_n), weight-average molecular weights (M_w), and dispersities ($Đ = M_w/M_n$) were calculated based on the system calibration and by assuming 100% mass elution from the columns using the Agilent GPC/SEC software.

Density functional theory (DFT) calculations. All-electron density functional theory (DFT) calculations were carried out using the NWChem suite of codes (version 7.2.1)[19] with the hybrid *meta* functional m06-2x[20] and the aug-cc-pvdz basis set.[21] Multiple S_N2 and addition–elimination reactions involving 1,5,7-Triazabicyclo[4.4.0]dec-5-ene (TBD), methanol (MeOH) and ethylene glycol (EG) with dimethyl carbonate (DMC) were considered. For each case, full geometry optimization was performed with tight convergence criteria. We explicitly computed the activation barrier (not corrected for zero-point energy) along the corresponding C–O bond of the complex formed by TBD—DMC and MeOH or EG connected at either the carbonyl group on DMC (addition–elimination) or the methyl (S_N2). Full geometry optimization was used at fixed bond lengths that increased in increments of 0.1 Angstroms. This reaction coordinate had an activation barrier with the computed energies (AE) and corresponding calculated transition states shown in Fig. S26–S30.

High performance liquid chromatography mass spectrometry. 5 μL sample was injected onto a Waters PAH C18 column (2 × 150 mm, 5 μm particle size; Waters Corp., Milford, MA, USA) for subsequent HPLC/MS analysis employing an Agilent 1100 HPLC system (Agilent Technologies, Santa Clara, CA, USA) coupled to a Q-Exactive HF orbitrap mass spectrometer (Thermo Scientific, Waltham, MA, USA). HPLC separation solvents A and B were 100/0.1 (v/v) water/FA and 100/0.1 (v/v) ACN/FA, respectively. The 14 min long gradient separation included the following steps: 0–2 min: 100% A; 2–3 min: linear gradient to 10% A; 3–5 min: linear gradient to 0% A; 5–8 min: 0% A, 8–8.1 min: linear gradient to 100% A; and 8.1–14 min: 100% A. Solution flow rate was 250 μL min^{-1}. Once the full mass spectrum was collected, the ten most abundant peaks were subjected to fragmentation using positive ion mode APCI. Exclusion time was set to 60 s to prevent fragmentation of the same ion in consecutive mass spectra. The APCI source had a set current of 4.0 μA, a capillary temperature of 300 °C, and a probe heater temperature of 300 °C. The nitrogen sheath gas and auxiliary gas were set to 60 and 30, respectively. Spare gas was not used. The S-lens of the instrument was set to 50 V. Full MS were acquired using scan range of m/z 50–700, resolution of 240 000, automatic gain control (AGC) target of 1 × 10^{6}, max injection time (IT) of 100 ms. Fragmentation spectra were acquired using a resolution of 15 000, AGC target of 5 × 10^{5}, max IT of 50 ms, and HCD energies of 30, 60 and 90 eV (three injections each about 17 ms) and averaged. Table S3 depicts detected *vs.* expected m/z for the oligoglycol ethers. Relevant mass spectra with m/z values indicated and compound structure are shown in Fig. S8. Compound assignments were made with the assistance of MSDial software.

Gas chromatography mass spectrometry. In a typical procedure, the solid sample was dissolved in dichloromethane at a concentration of 5 mg solids/gram solvent. The resulting solution was then directly injected into the GC/MS system which consisted of an Autosampler 7683 SERIES connected to an Agilent 6890N/5973 Network GC/MS system and the MS analysis focused on the m/z range of 10 to 200. CG-chromatograms and mass spectra are shown in Fig. S25.

Equations

Calculation of the selectivity of the deconstruction reaction in terms of the fraction of terephthalate esters derived from the alcohol or carbonate reagent used as determined *via* ^{1}H NMR spectroscopic analysis of the crude reaction mixtures, where I_{ester} is the integral area of the ester methylene/methyl protons of the desired product relative to all aromatic signals, which are set to $I = 1$, $n_{H,aromatic}$ is the number of expected aromatic protons of the product (*i.e.*, $n = 4$ for all terephthalate compounds), and $n_{H,ester}$ is the number of expected protons of the α-methylene/methyl carbon (*i.e.*, $n = 6$ for **DMT** and $n = 4$ for all other terephthalate compounds).

$$\%\,\text{Selectivity} = I_{ester}\frac{n_{H,aromatic}}{n_{H,ester}} \times 100\% \quad (1)$$

Calculation of deconstruction reaction conversion *via* gravimetric analysis, where m is the mass of PET remaining after the reaction and m_0 is the initial mass of PET used.

$$\%\,\text{Conversion} = \left(\frac{m}{m_0}\right) \times 100\% \quad (2)$$

Calculation of the yield of **EC** after deconstruction as determined *via* ^{1}H NMR spectroscopic analysis of the crude reaction mixtures, where I_{EC} is the integral area of the methylene protons of **EC** relative to all aromatic signals, which are set to $I = 1$, and %Conversion is defined by eqn (2).

$$\%\text{Yield}_{EC} = I_{EC} \times \%\text{Conversion} \quad (3)$$

Calculation of the fraction of **EC** formed during the reaction of EG and 5 equiv. of dimethyl carbonate in the presence of 1 mol% TBD relative to other carbonate and ether species. The integral area of **EC**, I_{EC}, was set to 1, with $I_{carb.}$ and I_{ether} representing the total integrated areas of the other formed carbonate species and ether species, respectively.

$$F_{EC} = \frac{I_{EC}}{I_{EC} + I_{carb.} + I_{ether}} \quad (4)$$

Calculation of the relative ratio of ethers formed during the reaction of EG and 5 equiv. of diethyl carbonate in the presence of 1 mol% TBD. The integral area of **EC**, I_{EC}, was set to 1, with $I_{carb.}$ and I_{ether} representing the total integrated areas of the other formed carbonate species and ether species, respectively.

$$F_{ether} = \frac{I_{ether}}{I_{EC} + I_{carb.} + I_{ether}} \quad (5)$$

Results and discussion

Catalyst selection for carbonate-mediated deconstruction

Initially, we sought to identify catalysts to promote PET deconstruction by transesterification and consumption of the evolving EG by irreversible alkylation. The efficacy of various Brønsted catalysts, ionic liquids, and Lewis catalysts, all of which are known catalyze transesterification reactions,[22] were investigated using dimethyl carbonate (DMC) as the reaction medium (Scheme S1). In addition to its unique reactivity, DMC is an abundant "green solvent" that can be sourced from biomass or CO_2.[23,24] In a typical experiment, PET pellets (weight average molecular weight, M_w = 46 kg mol^{-1}) were suspended in excess DMC (15 wt/v%) in the presence of 10 mol% catalyst and heated at 180 °C in a sealed pressure tube for 2 h. PET conversion was determined by gravimetric analysis and the selectivity of **DMT** formation was quantified *via* ^{1}H NMR spectroscopic analysis of the crude reaction mixtures (see eqn (1) and (2)). We observed quantitative consumption of PET with concomitant formation of **DMT** with each tested Brønsted base (Table 1, entries 1–4 and 7) catalyst except Hünig's base (*N*,*N*-diisopropylethylamine), which we attributed to its relatively weak basicity and poor nucleophilicity (Table 1, entry 8). The ionic liquid catalysts 1-butyl-3-methyl imidazolium (Bmim) [Bmim][OAc] and [Bmim][Cl] also mediated quantitative conversion of PET to **DMT** (Table 1, entries 5 and 6). In contrast, Brønsted and Lewis acid catalysts afforded low conversions of PET and only trace formation of the desired product **DMT** (Table 1, entries 10–12).

Next, we carefully analyzed the ^{1}H NMR spectra to determine the impact of catalyst identity on the consumption of the EG byproduct (see eqn (3)). Previous studies have shown that EG can be readily converted to ethylene carbonate, **EC**, in the presence of DMC.[18] However, this alone is not sufficient to alter the transesterification equilibrium, as EG can be regenerated from **EC** *via* subsequent transcarbonylation reactions. We sought catalysts that would further convert **EC** to oligoethers *via* alkylation, as indicated by the absence of both EG and **EC** after the deconstruction reaction. We found that superbase catalysts (*i.e.*, 1,5,7-triazabicyclo[4.4.0]decene (TBD) and its derivatives) afforded the lowest yields of **EC**, signifying its conversion into poly(ether carbonate) oligomers.[25] As such, TBD and its derivatives TBD/trifluoroacetic acid (TFA) and 7-methyltriazabicyclodecene (mTBD) were selected for further study (Table 1, entries 1–3).

Transesterification equilibria

With the optimum catalyst manifold determined, we next sought to compare the equilibrium behavior of PET deconstruction in the presence of various alcohols or carbonates selected to enable direct comparisons (see Table S1 for additional details). A series of experiments were conducted using different volumes of alcohol or carbonate reagent as the reaction medium at 180 °C for 24 h to ensure equilibration (Fig. 2A and Fig. S1). TBD/TFA (10 mol%) was used as the catalyst for these experiments due to its excellent thermal stability

Table 1 Catalyst optimization for CID

Entry	Catalyst	Classification	PET conversion[a] (%)	Selectivity[b] (%)	EC yield[c] (%)
1	TBD : TFA	Guanidine superbases	100	>99	45
2	TBD		100	>99	28
3	mTBD		100	>99	55
4	DMAP		100	>99	54
5	[Bmim][OAc]	Ionic liquids	100	>99	56
6	[Bmim][Cl]		100	>99	80
7	KO*t*Bu	Other Brønsted bases	100	>99	70
8	DIPEA		1	0	0
9	K_2CO_3		1	0	0
10	$Zn(OAc)_2$	Lewis acid	27	13	0.02
11	TsOH	Brønsted acids	2	0	0
12	H_2SO_4		3	0	0

[a] PET conversion was determined *via* gravimetric analysis. [b] Product selectivity was determined *via* ^{1}H NMR spectroscopic analysis. [c] **EC** yield was determined *via* ^{1}H NMR spectroscopic analysis of the crude reaction mixture. These experiments were carried out with 0.5 g of PET suspended in 15 wt/v% of DMC with 10 mol% of the appropriate catalyst at 180 °C for 2 h.

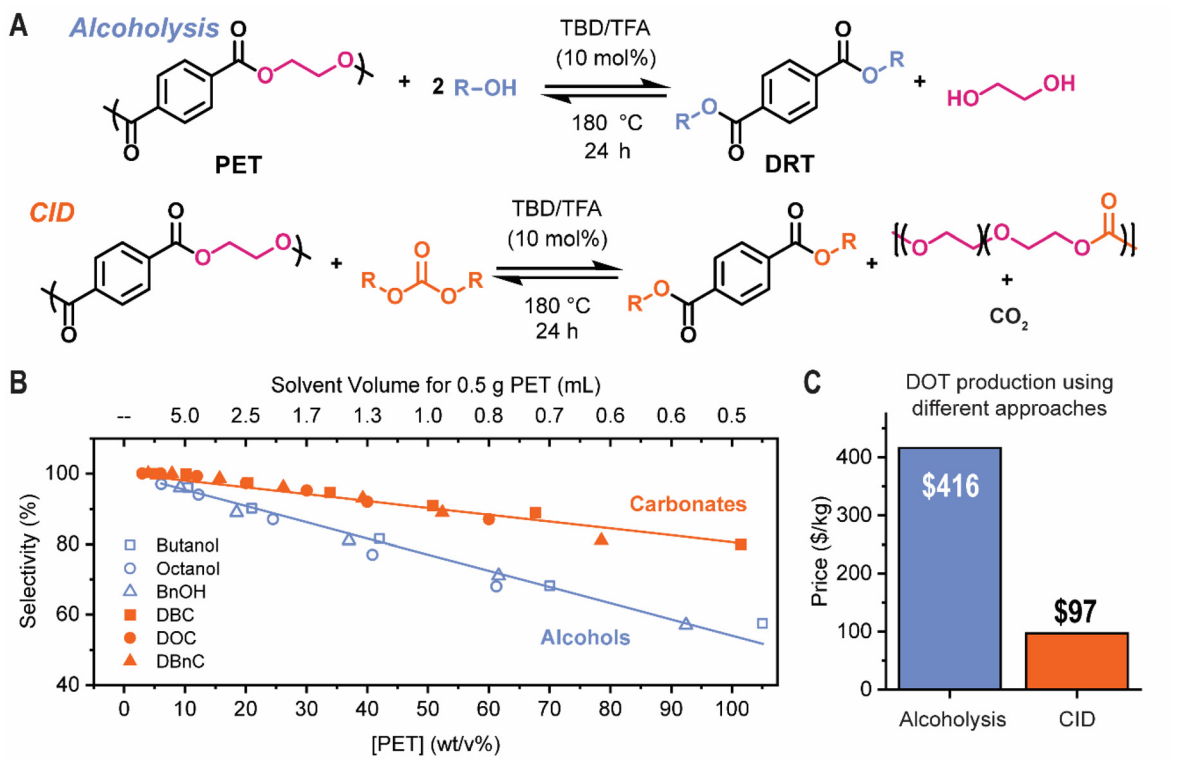

Fig. 2 (A) Schematic depicting the preparation of difunctional terephthalates using alcohols or carbonates as the reaction medium and source of nucleophile. (B) Plot of transesterification selectivity as a function of PET concentration for the various alcohols (orange closed symbols) and carbonates (blue open symbols). The solids lines represent concatenated linear fits of the alcohol and carbonate data. (C) Preliminary technoeconomic analysis derived from 0.5 g scale PET deconstructions using either 1-octanol or DOC as the solvent.

over long reaction times.[26] We note that PET was fully consumed in each trial as judged gravimetrically, even with just 1 molar equiv. of added reagent. After completion, an aliquot of each reaction mixture was removed and diluted in $CDCl_3$ for ^{1}H NMR spectroscopic analysis. Product selectivity, in terms of the percentage of terephthalate esters derived from the alcohol or carbonate, was determined *via* relative integration of the aromatic signals to those of the methylene protons adjacent to the terephthalate ester motifs (see eqn (1)). As shown in Fig. 2B, the selectivity of transesterification when using alcohols decreased rapidly with decreasing reagent volume (increasing PET concentration). In stark contrast, deconstructions mediated by carbonates were far less sensitive to stoichiometry and maintained good selectivity even at high PET concentration. Selectivities of 80%, 87%, and 81% were achieved when using just 1 molar equiv. of dibutyl carbonate

(DBC), dioctyl carbonate (DOC), or dibenzyl carbonate (DBnC), respectively, compared to just 58%, 68%, and 57% for butanol, octanol, and benzyl alcohol (BnOH).

To further illustrate the advantage of our methodology, we conducted a preliminary technoeconomic analysis (TEA) of CID compared to alcoholysis based on the conditions used for determining product equilibrium. We selected DOC and 1-octanol as the substrates of choice for this analysis. To achieve ~99% product selectivity and thus molar conversion at 0.5 g scale of PET, a vast excess of 1-octanol (50 mL) was required in contrast to the carbonate congener (4.2 mL). This significant solvent excess was needed to combat the alcoholysis equilibria and resulted in a stark 4× increase in material costs for alcoholysis as compared with CID (Fig. 2C, see SI for more details). Taken together, these data demonstrate that carbonates are highly advantaged for PET deconstruction by transesterification when compared to alcohols, facilitating good selectivity with minimal to no stoichiometric excess.

Mechanistic considerations

We sought to understand the mechanistic underpinnings of the observed high selectivity of CID using model experiments. Ethylene glycol monobenzoate (EGBz) and octyl benzoate (OBz) were subjected to 2 molar equiv. of DMC in the presence of 10 mol% TBD/TFA at 180 °C for 1 h. Methyl benzoate (MBz) was produced with 86% selectivity when starting from EGBz, while a lower selectivity of 58% was obtained from OBz (Fig. S2). The key difference between these two experiments was the presence or absence of EG, which drove the transesterification equilibrium *via* its conversion to oligoethers. Small molecule PET surrogates were further employed to interrogate the involvement of PET hydroxyl end groups in the deconstruction mechanism. Ethylene glycol dibenzoate (EGDBz) and EGBz were treated with 5 molar equiv. of DMC and 10 mol% TBD/TFA at 180 °C for 1 h. Quantitative conversion to MBz was observed for both PET analogues (Fig. S2). These results implicated acyl transfer reactions, mediated by the catalyst, in generating an initial fraction of nucleophilic alcoholic species required for transesterification.[27]

Kinetic monitoring was employed to follow the time-dependent consumption of PET relative to the formation of the key byproduct **EC** (from EG). Experiments were carried out in parallel using 10 mol% of either TBD, TBD/TFA, or mTBD and 5 molar equiv. of DMC at 180 °C and stopped at specified time points by removing the reaction vessels from heat. Aliquots of these mixtures were subjected to ^{1}H NMR spectroscopic analysis to track the formation of **EC**, while PET conversion was determined *via* gravimetric analysis on the recovered PET solids. Kinetic studies using TBD/TFA or mTBD exhibited notable induction periods during the first 10 min, with nearly quantitative PET mass recovery at these timepoints (Fig. S3). PET conversion increased rapidly after these induction periods, accompanied by increased evolution of **EC**. PET was completely consumed by 25 min and **EC** yield increased up to 0.55 molar equiv. relative to the terephthalate product. Prolonged reaction times affected a significant decrease in the quantity of **EC**, to <0.2 molar equiv., consistent with its consumption *via* polymerization.[28] Extending this kinetic investigation to TBD revealed similar trends, but on a much faster time scale and with no apparent induction period. In this system, complete PET consumption was observed within 10 min concomitant with **EC** formation and consumption.

A more in-depth kinetic analysis was conducted to monitor the consumption and formation of all key species (Fig. 3A). DOC was used for this experiment due to the low volatility of DOC itself and its constituent alcohol, 1-octanol. This factor allowed for its terminal methyl motifs to be used as an internal standard. TBD was used as the catalyst based on its relatively higher activity compared with TBD/TFA or mTBD. As before, each time point was represented by an individual reaction, with conversion values calculated from a combination of ^{1}H NMR spectroscopic and gravimetric analyses. As shown in Fig. 3B, **DOT** formation was commensurate with the consumption of both PET and DOC. Approximately 1 of the 5 molar equiv. of DOC was consumed (*i.e.*, 20%), suggesting that each equiv. of carbonate supplied the necessary 2 equiv. of alcohol to form the diester product. These processes occurred in tandem with **EC** formation and consumption, with **EC** concentration reaching a maximum at *ca.* 40 min before decreasing. Notably, the concentration of 1-octanol, derived from reaction with DOC, remained consistently low throughout the course of the reaction and was on the same order as the loading of TBD.

CID involves reactions between alcohols and carbonates *via* several distinct pathways. These pathways are highlighted in Fig. 3A. Briefly, EG released from PET or alcohol from the carbonate can both participate in intermolecular carbonylation ($B_{AC}2$) or methylation ($B_{AL}2$) reactions, while the asymmetric carbonate product can undergo an additional intramolecular carbonylation reaction to form **EC**. DFT computed activation energies for these various pathways revealed a slight kinetic preference for $B_{AC}2$ reactions involving EG, with the intramolecular reaction exhibiting the lowest barrier (Fig. S26–S30).

To confirm the liberation of CO_2 during CID, we first performed qualitative experiments utilizing bromothymol blue, a colorimetric indicator that is frequently used to detect the presence of carbonic acid. We bubbled the reaction headspace of a PET deconstruction reaction in the presence of DOC and TBD into a bromothymol blue solution. After 8 min, the solution turned bright yellow, supporting the evolution of CO_2 (Fig. 3C and Fig. S4). Further confirmation was provided *via* bubbling the reaction atmosphere into a limewater solution ($Ca(OH)_2$ in H_2O), which resulted in the precipitation of insoluble $CaCO_3$. Following these qualitative experiments, we turned our attention to quantify the amount of CO_2 released throughout the deconstruction. Analogous deconstruction reactions were conducted, and the headspace was analyzed *via* GC-MS, which indicated *ca.* 180 μmol of CO_2 was present after 2 h, >3× higher than was observed for a comparative reaction conducted with no added PET (Fig. 3D).

To assess **EC** polymerization, we conducted additional reactions where EG was used in place of PET. EG was almost fully converted to **EC** (>95%) within 2 min when reacted with 5 molar equiv. of diethyl carbonate (DEC) and 1 mol% TBD at

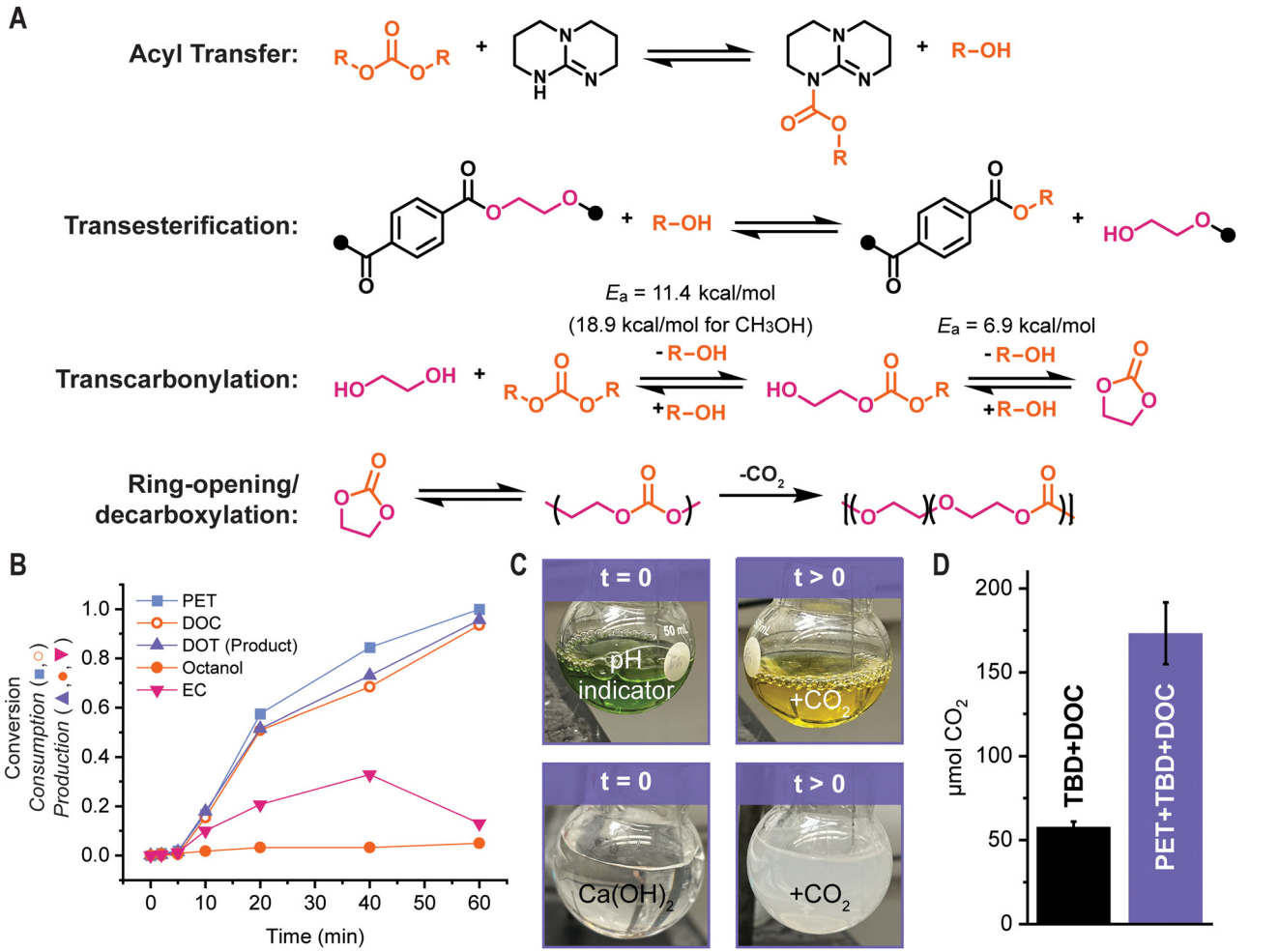

Fig. 3 (A) Highlighted key reaction pathways during CID. DFT computed activation energies are shown for the steps of the transcarbonylation pathways involving carbonate. DMC was used as the carbonate for these calculations. (B) Kinetic monitoring of PET deconstruction in the presence of 5 molar equiv. of DOC and 10 mol% TBD at 180 °C. Conversion values were calculated from gravimetric analysis or ^{1}H NMR spectroscopy. (C) Qualitative determination of CO_2 formation using a pH indicator or by precipitation of $CaCO_3$. (D) Quantitative determination of CO_2 formed during CID *via* sampling of the reaction headspace followed by MS analysis to determine the μmol of CO_2 produced.

180 °C. The generated **EC** was then consumed in pseudo-first-order fashion over the next 58 min (Fig. S5), resulting in the formation of various carbonate and ether species as judged by ^{1}H NMR spectroscopy (Fig. S6). **EC** consumption was accompanied by a gradual shift in the ratio of ether and carbonate products, consistent with the conversion of carbonates to ethers *via* decarboxylation (Fig. S7). High resolution mass spectrometry (HRMS) analysis of a similar reaction between EG and DOC that was left open to air at 180 °C for 24 h to promote CO_2 off-gassing confirmed the formation of various glycol ether products, including tetraethylene and hexaethylene glycol, diethylene glycol monooctyl ether, and 18-crown-6 ether (Table S3 and Fig. S8).

Based on our findings from model reactions and kinetic experiments, and considering the reported reactivity of carbonates in the chemical literature,[18] the following conclusions regarding the mechanism of CID were drawn: (1) the catalyst (*i.e.*, TBD) was responsible for the generation of free nucleophile *via* acyl transfer, and the concentration of free nucleophile was proportional to catalyst loading throughout the course of the reactions; (2) both acyl transfer and proton transfer catalysis were in operation simultaneously, with the former providing faster overall reaction kinetics; (3) EG generated by transesterification with PET was rapidly converted to **EC** *via* reaction with carbonate and subsequent intramolecular cyclization; and (4) **EC** was polymerized in the later stages of the reaction to form poly(carbonate)s, which were gradually converted to polyethers *via* transalkylcarbonylation coincident with the generation of CO_2. The irreversibility of this final process drove the selectivity of the CID reactions, ultimately suppressing glycolated byproduct formation *via* the removal of EG from the reaction equilibrium.

Carbonate scope exploration

Based on the success of PET deconstruction using carbonates, we anticipated that a library of valuable terephthalate products

could be accessed from plastic waste by employing carbonates with diverse functionality. Symmetrical carbonates such as diethyl, dibutyl, dioctyl, diallyl and dibenzyl carbonate were selected due to their liquid form, commercial availability, and value of the resulting terephthalate product. It should be noted that these carbonates can be prepared sustainably *via* CO_2 and the appropriate alcohol.[28,29] With these targets in mind, we assessed if the PET deconstruction selectivity achieved using these carbonates would be comparable to our initial experiments. A series of PET deconstructions were conducted using fixed reaction stoichiometry and temperature and varying the carbonate used (10 mol% TBD, PET pellets suspended in 5 molar equiv. of the respective carbonate, 180 °C). We observed quantitative conversion of PET and concomitant formation of **DMT**, diethyl terephthalate (**DET**), **DAT**, or **DBnT** as the sole terephthalate product within 20 min when their corresponding carbonates were used (Fig. 4A). While similar conversions and yields were observed with DBC or DOC, longer deconstruction times (2 h) were required. The resulting terephthalate products could be easily isolated from the deconstruction reaction mixtures *via* recrystallization or chromatography, affording good isolated yields.

With the library of terephthalate products in hand, we sought to demonstrate how their embedded reactive motifs could be further elaborated to access other high value terephthalates that cannot be prepared directly from PET due to various side reactions at elevated temperature.[30] We identified a simple two-step pathway to synthesize diglycidyl terephalate (**DGT**) *via* the functional intermediate **DAT**. In a typical experiment, a transparent PET egg carton was cut into rectangular slices and deconstructed to **DAT** using our standard conditions. **DAT** was isolated in 92% yield from the crude reaction mixture *via* flash column chromatography. **DAT** from PET waste was then subjected to mild epoxidation conditions with excess *meta*-Chloroperbenzoic acid (*m*-CPBA) at 40 °C (Fig. 4B), after which **DGT** was isolated as a white powder in 70% yield, or in 65% overall yield starting from PET.

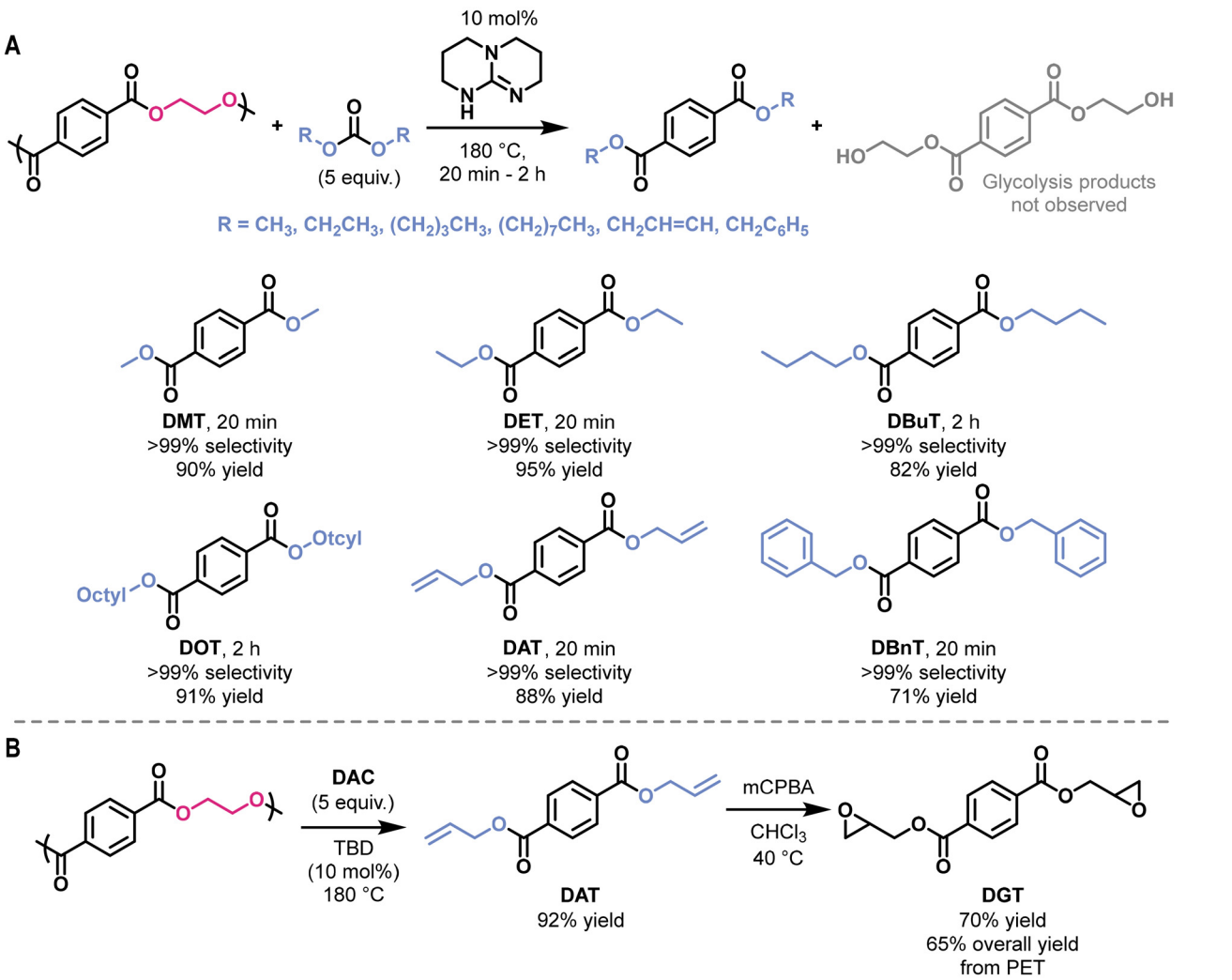

Fig. 4 (A) High value terephthalate products accessible *via* CID. Reaction conversions and isolated yields are shown below each synthesized compound. (B) Synthesis of diglycidyl terephthalate (**DGT**) in two steps starting from PET egg carton waste.

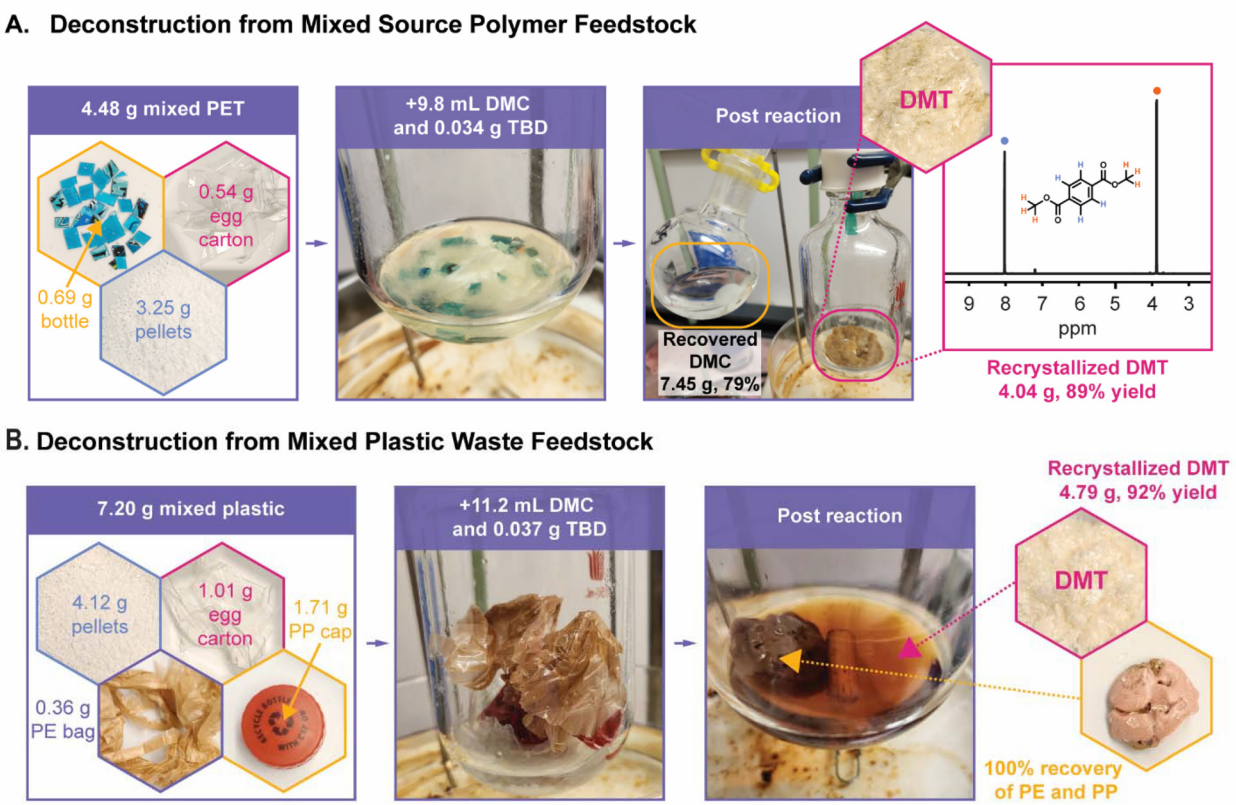

Fig. 5 Scale-up deconstruction of a mixture of (A) PET from various sources and (B) mixed plastic waste, highlighting the robustness and simplicity of this methodology, the minimal excess of carbonate, the good recoverability of the carbonate after reaction, and the high yield and purity of the desired terephthalate product.

Demonstration using mixed PET waste

To demonstrate the deployability of this methodology and its tolerance of the various impurities present in post-consumer plastic waste, we performed a deconstruction reaction using a mixture of pristine PET (3.25 g), a PET water bottle (0.69 g of chopped pieces), and a PET egg carton (0.54 g of chopped pieces). This mixture was suspended in DMC (5 molar equiv.) in a sealed pressure tube and heated to 180 °C in the presence of 1 mol% TBD for 3.5 h (Fig. 5A). After cooling to room temperature, the un-reacted DMC was recovered *via* distillation (79% of the total mass used), and the resulting solid residue was recrystallized from MeOH to afford **DMT** in good purity and yield (89%, Table S4) as confirmed by ^{1}H NMR (Fig. 5A) and gas-chromatography mass spectrometry analysis (Fig. S25). This selective deconstruction eliminated the need for upfront separation and cleaning of the mixed plastic waste and enabled *ca.* 4.5 g of PET from various sources to be directly converted to **DMT** using just 9.8 mL of carbonate and 0.034 g of catalyst.

We also attempted CID staring from a mixed plastic waste feedstock (Fig. 5B). Pristine PET (4.12 g), a PET egg carton (1.01 g), a PE grocery bag (0.36 g), and a PP cap from a soda bottle (1.74 g) were suspended in 5 molar equiv. of DMC and 1 mol% TBD. After heating in a sealed pressure tube at 180 °C for 4 h, the **DMT** product was easily separated from the other plastic impurities *via* a simple 4-step process involving dilution with tetrahydrofuran, filtration, concentration, and recrystallization from MeOH. As above, **DMT** was obtained in high isolated yield (92%) and good purity and minimal DMC (11.2 mL) and TBD (0.037 g) were used.

Conclusion

In summary, we have shown that PET was successfully upcycled by CID in the presence of nucleophilic catalysts to afford valuable organic terephthalates. This methodology enabled precise control over transesterification equilibria, favoring the formation of a single terephthalate product over glycolated byproducts as supported through DFT calculations and model and kinetic experiments. A library of carbonates was demonstrated to be amenable to this strategy, affording a variety of useful organic compounds that could be elaborated further to access terephthalates with privileged architectures inaccessible through direct alcoholysis. CID was also extended to post-consumer mixed plastic waste, demonstrating the resiliency of this method to the various impurities and contaminants commonly encountered therein. Our results highlight

the many advantages of using carbonates over traditional alcohols in the deconstruction of condensation polymers, including high selectivity, good yields and low solvent loading. We anticipate that this platform offers a robust foundation for the development of advanced deconstruction products from various condensation polymer waste streams and can facilitate a circular carbonate economy in which CO_2 captured from the environment and other various processes, can be converted to symmetric carbonate solvents and further leveraged to choreograph the selectivity of otherwise equilibrium-controlled deconstruction processes.

Author contributions

Nicholas J. Galan: conceptualization, investigation, methodology, visualization, writing (original draft & editing). Isaiah T. Dishner: investigation, writing (review & editing). Bobby Sumpter: investigation, funding acquisition, writing (review & editing). Vilmos Kertesz: investigation, writing (review & editing). Nabihan B. Abdul Rahman: investigation, writing (review & editing). Felipe Polo-Garzon: investigation, writing (review & editing). Zoriana Demchuk: investigation, writing (review & editing). Tomonori Saito: conceptualization, supervision, funding acquisition writing (review & editing). Jeffrey C. Foster: conceptualization, funding acquisition, investigation, methodology, visualization, writing (original draft & editing).

Conflicts of interest

The authors declare no competing interests.

Data availability

The data supporting this article have been included as part of the SI. Supplementary information is available. See DOI: https://doi.org/10.1039/d5gc03354c.

Acknowledgements

The authors thank Dr Ilja Popovs and Dr Jared Bowman for invaluable discussion. This research was primarily supported by the US Department of Energy, Office of Science, Basic Energy Sciences, Materials Sciences and Engineering Division. GC-MS characterization was supported by the US Department of Energy, Office of Science, Office of Basic Energy Sciences, Chemical Sciences, Geosciences, and Biosciences Division, Catalysis Science program. DFT calculations were performed at the Center for Nanophase Materials Sciences, a US Department of Energy Office of Science User Facility operated at Oak Ridge National Laboratory.

References

1 *Polycarbonate Market Size, Share & Trends Analysis Report By Application (Automotive & Transportation, Electrical & Electronics, Construction, Packaging, Consumer Goods), By Region, And Segment Forecasts, 2023–2030*, Grand View Research, San Francisco, CA, 2022.
2 *Polyester Fiber Market Size, Share & Trends Analysis Report By Type (Polyester Staple Fiber, Polyester Filament Yarn), By Source, By Grade, By Form, By Denier, By Application, By Region, And Segment Forecasts, 2024–2030*, Grand View Research, San Francisco, CA, 2023.
3 *Polyamide Market Size, Share & Trends Analysis Report By Product (Polyamide 6, Polyamide 66, Bio-based Polyamide, Specialty Polyamides), By Application (Engineering Plastics, Fibers), By Region, And Segment Forecasts, 2021–2028*, Grand View Research, San Francisco, CA, 2021.
4 *Polyurethane Market Size, Share & Trends Analysis Report By Raw Material (Toluene Di-isocyanate, Methylene Diphenyl Di-isocyanate, Polyols), By Product, By Application, By Region, And Segment Forecasts, 2024–2030*, Grand View Research, San Francisco, CA, 2023.
5 N. Van Camp, I. S. Lase, S. De Meester, S. Hoozée and K. Ragaert, Exposing the pitfalls of plastics mechanical recycling through cost calculation, *Waste Manag.*, 2024, **189**, 300–313.
6 PlasticsEurope. PlasticsEurope, 2023, Available from: https://plasticseurope.org/knowledge-hub/plastics-the-fast-facts-2023/.
7 J. Zheng, M. Arifuzzaman, X. Tang, X. C. Chen and T. Saito, Recent development of end-of-life strategies for plastic in industry and academia: bridging their gap for future deployment, *Mater. Horiz.*, 2023, **10**(5), 1608–1624.
8 A. Rahimi and J. M. García, Chemical recycling of waste plastics for new materials production, *Nat. Rev. Chem.*, 2017, **1**(6), 0046.
9 X. Chen, Y. Wang and L. Zhang, Recent Progress in the Chemical Upcycling of Plastic Wastes, *ChemSusChem*, 2021, **14**(19), 4137–4151.
10 C. Jehanno, J. W. Alty, M. Roosen, S. De Meester, A. P. Dove, E. Y. X. Chen, *et al.*, Critical advances and future opportunities in upcycling commodity polymers, *Nature*, 2022, **603**(7903), 803–814.
11 S. Westhues, J. Idel and J. Klankermayer, Molecular catalyst systems as key enablers for tailored polyesters and polycarbonate recycling concepts, *Sci. Adv.*, 2018, **4**(8), eaat9669.
12 S. Lu, Y. Jing, B. Feng, Y. Guo, X. Liu and Y. Wang, H2-free Plastic Conversion: Converting PET back to BTX by Unlocking Hidden Hydrogen, *ChemSusChem*, 2021, **14**(19), 4242–4250.
13 A. D. Godwin, 26 – Plasticizers, in *Applied Plastics Engineering Handbook*, ed. M. Kutz, William Andrew Publishing, aaaa, 3rd edn, 2024, pp. 595–618.
14 Ö. Gök, Didodecyl terephthalate, ditetradecyl terephthalate, and dioctadecyl terephthalate compounds as novel phase

change materials for medium temperature applications, *J. Energy Storage*, 2022, **56**, 105859.
15 K. W. J. Ng, J. S. K. Lim, N. Gupta, B. X. Dong, C.-P. Hu, J. Hu, *et al.*, A facile alternative strategy of upcycling mixed plastic waste into vitrimers, *Commun. Chem.*, 2023, **6**(1), 158.
16 J. C. Foster, J. Zheng, M. Arifuzzaman, M. A. Rahman, J. T. Damron, C. Guan, *et al.*, Closed-loop recycling of semi-aromatic polyesters upcycled from poly(ethylene terephthalate), *Cell Rep. Phys. Sci.*, 2023, **4**, 101734.
17 J. Otera, Transesterification, *Chem. Rev.*, 1993, **93**(4), 1449–1470.
18 P. Tundo and M. Selva, The Chemistry of Dimethyl Carbonate, *Acc. Chem. Res.*, 2002, **35**(9), 706–716.
19 M. Valiev, E. J. Bylaska, N. Govind, K. Kowalski, T. P. Straatsma, H. J. J. Van Dam, *et al.*, NWChem: A comprehensive and scalable open-source solution for large scale molecular simulations, *Comput. Phys. Commun.*, 2010, **181**(9), 1477–1489.
20 Y. Zhao and D. G. Truhlar, A new local density functional for main-group thermochemistry, transition metal bonding, thermochemical kinetics, and noncovalent interactions, *J. Chem. Phys.*, 2006, **125**(19), 194101.
21 T. H. Dunning Jr, Gaussian basis sets for use in correlated molecular calculations. I. The atoms boron through neon and hydrogen, *J. Chem. Phys.*, 1989, **90**(2), 1007–1023.
22 S. C. Kosloski-Oh, Z. A. Wood, Y. Manjarrez, J. P. de los Rios and M. E. Fieser, Catalytic methods for chemical recycling or upcycling of commercial polymers, *Mater. Horiz.*, 2021, **8**(4), 1084–1129.
23 S.-H. Pyo, J. H. Park, T.-S. Chang and R. Hatti-Kaul, Dimethyl carbonate as a green chemical, *Curr. Opin. Green Sustainable Chem.*, 2017, **5**, 61–66.
24 A. Raza, M. Ikram, S. Guo, A. Baiker and G. Li, Green Synthesis of Dimethyl Carbonate from CO2 and Methanol: New Strategies and Industrial Perspective, *Adv. Sustainable Syst.*, 2022, **6**(8), 2200087.
25 J.-C. Lee and M. H. Litt, Ring-Opening Polymerization of Ethylene Carbonate and Depolymerization of Poly(ethylene oxide-co-ethylene carbonate), *Macromolecules*, 2000, **33**(5), 1618–1627.
26 M. Arifuzzaman, B. G. Sumpter, Z. Demchuk, C. Do, M. A. Arnould, M. A. Rahman, *et al.*, Selective deconstruction of mixed plastics by a tailored organocatalyst, *Mater. Horiz.*, 2023, **10**(9), 3360–3368.
27 R. C. Pratt, B. G. G. Lohmeijer, D. A. Long, R. M. Waymouth and J. L. Hedrick, Triazabicyclodecene: A Simple Bifunctional Organocatalyst for Acyl Transfer and Ring-Opening Polymerization of Cyclic Esters, *J. Am. Chem. Soc.*, 2006, **128**(14), 4556–4557.
28 H. Mutlu, J. Ruiz, S. C. Solleder and M. A. R. Meier, TBD catalysis with dimethyl carbonate: a fruitful and sustainable alliance, *Green Chem.*, 2012, **14**(6), 1728–1735.
29 W. S. Putro, A. Ikeda, S. Shigeyasu, S. Hamura, S. Matsumoto, V. Y. Lee, *et al.*, Sustainable Catalytic Synthesis of Diethyl Carbonate, *ChemSusChem*, 2021, **14**(3), 842–846.
30 Due to the incompatibility of various functional groups such as epoxides with the conditions of PET deconstruction.

